Validating and modeling the impact of high-frequency rapid antigen screening on COVID-19 spread and outcomes

Authors: Beatrice Nash[1,2*], Anthony Badea[1,3*], Ankita Reddy[1,4*], Miguel Bosch[1,5], Nol Salcedo[1], Adam R. Gomez[1], Alice Versiani[6], Gislaine Celestino Dutra Silva[6], Thayza Maria Izabel Lopes dos Santos[6], Bruno H. G. A. Milhim[6], Marilia M Moraes[6], Guilherme Rodrigues Fernandes Campos[6], Flávia Quieroz[6], Andreia Francesli Negri Reis[6], Mauricio L. Nogueira[6], Elena N. Naumova[7], Irene Bosch[1,8], Bobby Brooke Herrera[1,9†]

[*]These authors contributed equally to this work.

Affiliations:

[1]E25Bio, Inc., Cambridge, MA, USA

[2]Department of Computer Science, Harvard University School of Engineering and Applied Sciences, Cambridge, MA, USA

[3]Department of Physics, Harvard University, Cambridge, MA, USA

[4]Perelman School of Medicine, University of Pennsylvania, Philadelphia, PA, USA

[5]InfoGeosciences LLC, Houston, TX, USA

[6]Faculdade de Medicina de São José do Rio Preto (FAMERP), São José do Rio Preto, Brazil

[7]Division of the Nutrition Epidemiology and Data Science, Friedman School of Nutrition Science and Policy, Tufts University, Boston, MA, USA

[8]Department of Medicine, Mount Sinai School of Medicine, New York, NY, USA

[9]Department of Immunology and Infectious Diseases, Harvard T.H. Chan School of Public Health, Boston, MA, USA

[†]Corresponding Author. BBH, email: bbherrera@e25bio.com

Short Title: Modeling rapid antigen testing on COVID-19 spread

Abstract

High frequency screening of populations has been proposed as a strategy in facilitating control of the COVID-19 pandemic. We use computational modeling, coupled with clinical data from rapid antigen tests, to predict the impact of frequent viral antigen rapid testing on COVID-19 spread and outcomes. Using patient nasal or nasopharyngeal swab specimens, we demonstrate that the sensitivity/specificity of two rapid antigen tests compared to quantitative real-time polymerase chain reaction (qRT-PCR) are 82.0%/100% and 84.7%/85.7%, respectively; moreover, sensitivity correlates directly with viral load. Based on COVID-19 data from three regions in the United States and São José do Rio Preto, Brazil, we show that high frequency, strategic population-wide rapid testing, even at varied accuracy levels, diminishes COVID-19 infections, hospitalizations, and deaths at a fraction of the cost of nucleic acid detection via qRT-PCR. We propose large-scale antigen-based surveillance as a viable strategy to control SARS-CoV-2 spread and to enable societal re-opening.

INTRODUCTION

The COVID-19 pandemic has taken an unprecedented toll on lives, wellbeing, healthcare systems, and global economies. As of 18 January 2021, there have been more than 95.2 million confirmed cases globally with more than 2 million confirmed deaths[1]. However, these statistics and the current mapping of disease spread present an incomplete picture of the outbreak largely due to the lack of adequate testing, particularly as undetected infected cases are the main source of disease spread [2–7]. It is estimated that the number of infected cases is more than 6 times higher than the cases reported[8]. As of January 2021, the United States, India, and Brazil remain the top three countries with the highest number of COVID-19 cases and deaths worldwide. As countries begin to re-open their economies, a method for accessible and frequent surveillance of COVID-19, with the necessary rapid quarantine measures, is crucial to prevent the multiple resurgences of the disease.

The current standard of care rightfully places a strong focus on the diagnostic limit of detection, yet frequently at the expense of both cost and turnaround time. This situation has contributed to limited population testing largely due to a dearth of diagnostic resources. Quantitative real-time polymerase chain reaction (qRT-PCR) is the gold-standard method for clinical diagnosis, with high sensitivity and specificity, but these tests require trained personnel, expensive reagents and instrumentation, and a significant amount of time to execute[9,10]. Facilities offering qRT-PCR sometimes require a week or longer to complete and return the results to the patient[11,12]. During this waiting period the undiagnosed individual may spread the infection and/or receive delayed medical treatment. Moreover, due to the cost and relative inaccessibility of qRT-PCR in both resource-limited and abundant settings, large-scale screening using qRT-PCR at frequent intervals remains impractical to identify infected but asymptomatic or mildly

92 symptomatic infections. Numerous studies have reported asymptomatic SARS-CoV-2 infections
93 as well as a variation in viral load within and between individuals at different time points,
94 suggesting the need for more frequent testing for informative surveillance[13–18].

95 Technologies such as rapid viral antigen detection, clustered regularly interspaced short
96 palindromic repeats (CRISPR), and loop-mediated isothermal amplification (LAMP) of SARS-
97 CoV-2 provide potential large-scale screening applications, yet their implementation is stymied by
98 requirements for qRT-PCR-like accuracy before they can reach the market [19]. Several members of
99 the scientific and medical community have emphasized the value of widespread and frequent
100 antigen testing[20–22]. In countries such as India, where the qRT-PCR resources would not be
101 sufficient to cover monitoring of the population, the use of rapid antigen tests is well underway[23,24].
102 In early May 2020, the United States Food and Drug Administration (FDA) authorized the first
103 antigen test for the laboratory detection of COVID-19, citing a need for testing beyond molecular
104 and serological methods. Antigen testing detects the viral proteins rather than nucleic acids or
105 human antibodies, allowing for detection of an active infection with relative ease of sample
106 collection and assay. These rapid assays – like other commercially-available rapid antigen tests -
107 can be mass-produced at low prices and be administered by the average person without a laboratory
108 or instrumentation. These tests also take as little as 15 minutes to determine the result, enabling
109 real-time surveillance and/or diagnosis. Although antigen tests usually perform with high
110 specificities (true negative rate), their sensitivity (true positive rate) is often lower when compared
111 to molecular assays. While qRT-PCR can reach a limit of detection as low as 10^2 genome copies
112 per mL, rapid antigen testing detects viral protein that is assumed to correlate with approximately
113 10^5 genome copies per mL [25].

We hypothesize that frequent antigen-based rapid testing even with lower sensitivities compared to qRT-PCR - along with appropriate quarantine measures - can be more effective at decreasing COVID-19 spread than less frequent molecular testing of symptomatic individuals. Keeping in mind the realities of daily testing in resource-limited regions, we also hypothesize that testing frequency can be adjusted according to the prevalence of the disease; that is, an uptick in reported cases should be accompanied by more frequent testing. During the viral incubation period, high infectivity correlates with a high viral load that can be detected by either qRT-PCR or rapid antigen testing [18,21,26–28]. Rapid tests thus optimize diagnosis for the most infectious individuals. Studies also point to the relatively small window of time during an individual's incubation period in which the qRT-PCR assay is more sensitive than rapid tests [21].

In this study we report the clinical validation of two direct antigen rapid tests for detection of SARS-CoV-2 spike glycoprotein (S) or nucleocapsid protein (N) using retrospectively collected nasopharyngeal or nasal swab specimens. Using the clinical performance data, we develop a modeling system to evaluate the impact of frequent rapid testing on COVID-19 spread and outcomes using a variation of a SIR model, which has been previously used to model COVID-19 transmission [29–35]. We build on this model to incorporate quarantine states and testing protocols to examine the effects of different testing regimes. This model distinguishes between undetected and detected infections and separates severe cases, specifically, those requiring hospitalization, from those less so, which is important for disease response systems such as intensive care unit triaging. We simulate COVID-19 spread with rapid testing and model disease outcomes in three regions in the United States and São José do Rio Preto, Brazil - the site of the clinical validation study - using publicly available data. To date, COVID-19 modeling describes the course of disease spread in response to social distancing and quarantine measures, and a previous simulation study has shown

137 that frequent testing with accuracies less than qRT-PCR, coupled with quarantine process and
138 social distancing, are predicted to significantly decrease infections [21,29,35–39]. This is the first
139 modeling system using publicly-available data to simulate how potential public health strategies
140 based on testing performance, frequency, and geography impact the course of COVID-19 spread
141 and outcomes. Our findings suggest that a rapid test, even with sensitivities lower than molecular
142 tests, when strategically administered 2-3 times per week, will reduce COVID-19 spread,
143 hospitalizations, and deaths at a fraction of the cost of nucleic acid testing via qRT-PCR. Modern
144 surveillance systems should be well equipped with rapid testing tools to ensure that disease
145 tracking and control protocols are effective and well-tailored to national, regional, and community
146 needs.
147

148 **RESULTS**

149 **Accuracy of Direct Antigen Rapid Tests Correlate with Viral Load Levels**

150 Rapid antigen tests have recently been considered a viable source for first-line screening,
151 although concerns regarding the accuracy of these tests persist. We clinically validated two
152 different direct antigen rapid tests for the detection of either N or S from SARS-CoV-2 in
153 retrospectively collected nasal or nasopharyngeal swab specimens. Of the total number of nasal
154 swab specimens evaluated by qRT-PCR for amplification of SARS-CoV-2 N, S, and ORF1ab
155 genes, 100 tested positive and 58 tested negative (Table 1-2). The overall sensitivity and specificity
156 of the rapid antigen test for detection of SARS-CoV-2 N, evaluated across the nasal swab
157 specimens, was 82.0% and 100%, respectively. Of the total number of nasopharyngeal swab
158 specimens evaluated by qRT-PCR for amplification of SARS-CoV-2 N, RNA-dependent RNA
159 polymerase (RdRp), and envelope (E) genes, 72 tested positive and 49 tested negative (Table 1,

160 Table 3). The overall sensitivity and specificity of the rapid antigen test for detection of SARS-
161 CoV-2 S, evaluated across the nasopharyngeal swab specimens was 84.7% and 85.7%,
162 respectively. Altogether, our data demonstrate that the sensitivity of the rapid antigen tests are
163 positively correlated to the viral load level (Table 1, Figure S1).

164 The Ct value indirectly quantifies the viral RNA copy number related to the viral load of
165 the sample for the specific assay [40–42]. Ct values represent the number of qRT-PCR cycles at which
166 generated fluorescence crosses a threshold during the linear amplification phase; Ct values are
167 therefore inversely related to the viral load. The sensitivity of both rapid antigen tests increases as
168 Ct value decreases (Table 1). Moreover, because the Ct value is a variable unit based upon qPCR
169 protocol and instrumentation, we evaluated sensitivity against the percentile of positive cases
170 conditioned to Ct and found similar results. The sensitivity of the rapid antigen test for detection
171 of SARS-CoV-2 N increased from 80.0% at Ct values <40 to 92.5% at Ct values <25
172 (Supplementary Fig. 1a). Similarly, the sensitivity of the rapid antigen test for detection of SARS-
173 CoV-2 S increased from 84.7% at Ct values <35 to 100.0% at Ct values <15 (Supplementary Fig.
174 1b). Taken together, the clinical data shows that the rapid antigen test performs with increasing
175 accuracy for individuals with a higher viral load, and potentially the most infectious [18,26–28].
176

177 **An Enhanced Epidemiological SIDHRE-Q Model**

178 We propose an enhanced epidemiological modeling system, *SIDHRE-Q,* a variant of the
179 classical SIR model in order to expand our clinical validation study and to understand the effects
180 of using frequent rapid tests such as the rapid antigen test on COVID-19 outbreak dynamics. The
181 changes we make to the basic model to encompass the unique characteristics of the COVID-19
182 pandemic are similar to those presented by Giordano et al. *(16)* (Fig. 1, Supplementary Fig. 2).

183 The differential equations governing the evolution of the *SIDHRE-Q* model and descriptions of
184 the parameter values are provided in the methods section (Equation 1, Table 4).

185 An individual that begins in Susceptible (**S)** may either transition to a Quarantine
186 Uninfected (**Q-U**) state via a false positive result or to an Infected Undetected (**I**) state via
187 interaction with an infected individual. Should an individual in **S** move into **Q-U**, they are
188 quarantined for 10 days before returning to **S**, a time period chosen based on current knowledge
189 of the infectious period of the disease and is consistent with CDC guidelines[43]. One could also
190 conceive of an effective strategy in which individuals exit quarantine after producing a certain
191 number of negative rapid tests in the days following their initial positive result or confirm their
192 negative result using qRT-PCR. Prolonged incubation beyond 10 days is assumed to be unlikely
193 – post-quarantine risk of transmission is estimated at 1% - and hence is not included in this
194 probabilistic model. [43]

195 State **I** contains individuals who are infected but not diagnosed. Given that those diagnosed
196 are predominantly quarantined, the undiagnosed individuals in **I** – many of which are pre- or
197 asymptomatic – interact more with the **S** population than do those in Infected Detected (**D**) and
198 transmission due to this population is critically important to modeling outbreaks. Therefore, the
199 infectious rate for **I** is assumed to be significantly larger than for **D**. Furthermore, a region's ability
200 to control an outbreak is directly related to how quickly and effectively the population in **I** tests
201 into **D**, reducing transmission rates through quarantine. From both **I** and **D** individuals may
202 transition into Recovered (**R)**, accounting for the many cases of infection that are never detected.
203 This study, in particular, highlights the critical role frequency of testing, along with strict
204 quarantine, has in mitigating the spread of the disease and provides specific testing strategies based
205 on rapid tests we predict to be highly effective.

In this model, we assume that individuals receive a positive diagnosis before developing severe symptoms and that those with symptoms severe enough to be potentially fatal will go to the hospital. If an individual develops symptoms, we assume they are tested daily until receiving a positive result; hence, before severe symptoms develop, they will be diagnosed with high probability. Those who do not develop symptoms are tested according to the frequency of tests administered to the general population. Therefore, there is no modeled connection between **I** and Hospitalized (**H)** or between **I** and Extinct (**E)**. Removing these assumptions would have negligible impact on the results as these flows are very small. We estimated the flows using data on approximate total deaths due to COVID based on excess deaths in the states examined and found them to be zero on greater than 10% of the days considered for each location. Although lacking this information for São José do Rio Preto, we made the same assumption.

Should an individual test positive and transition to **D**, they may either develop serious symptoms requiring care or recover. Those who develop serious symptoms and transition to state **H** will then transition to either **R** or **E**. The recovered population is also tested with the same frequency as the rest of the population, as infected individuals may recover without being detected and the modeled testing strategy has no way of differentiating with certainty between false positives and true positive, asymptomatic cases. Therefore, the Quarantined Recovered (**Q-R**) state is introduced with the same connections to **R** as the connections between **S** and **Q-U**. Though the reinfection rate of SARS-CoV-2 has been a point of recent debate, it is assumed that the number of re-infected individuals is small [44–48]. Therefore, individuals cannot transition from **R** to **S**, hence the separately categorized quarantined populations. Should knowledge to the contrary arise as the pandemic continues, a flow could be added from **R** to **S** with rate inversely proportional to the time for which immunity lasts.

We considered several variations and extensions of the *SIDHRE-Q* model. In simulations, we tested additional states, such as those in the *SIDARTHE* model, which include distinctions between symptomatic and asymptomatic cases for both detected and undetected populations [29]. Incorporating information about the correlations between viral load and infectivity and sensitivity were also considered. Altogether, our modeling system has been well tuned to predict the impact of high frequency rapid testing on COVID-19 spread and outcomes.

Frequent Rapid Testing with Actionable Quarantining Dramatically Reduces Disease Spread

In order to demonstrate how strategies could affect the disease spread in different geographies and demographics, we used surveillance data obtained from regions of varying characteristics: the state of Massachusetts (MA), New York City (NYC), Los Angeles (LA), and São José do Rio Preto (SJRP), Brazil, the site of the rapid antigen test clinical validation study. These regions are also selected in our study due to the readily available surveillance data provided by the local governments. We fit the model to the data from each region starting 1 April 2020. At this time point the disease reportedly is most advanced in NYC and least advanced in SJRP, Brazil with estimated cumulative infection rates of 7.11% and 0.12%, respectively.

After calibrating the *SIDHRE-Q* model, the disease spread is observed with varying validated rapid antigen test performances and frequencies (Fig. 2). Sensitivity (the ratio of true positives to the total number of positives) and specificity (the ratio of true negatives to the total number of negatives) compared to gold-standard qRT-PCR were used as measures of test accuracy.

The rapid test frequency is varied while maintaining an accuracy of 80% sensitivity and 90% specificity, comparable to our clinical data collected in SJRP, Brazil. These testing scenarios are then compared to symptomatic testing, in which individuals receive a rapid test only when presenting symptoms, via either a rapid test or qRT-PCR. Since the primary testing regimen deployed in MA, LA, NYC and SJRP, Brazil is qRT-PCR-based and focused on symptomatic individuals, the symptomatic testing protocol via qRT-PCR is directly estimated from the data to be the rate ν (Table 4).

The difference between the qRT-PCR and rapid test simulations (red and orange lines, respectively) is therefore only sensitivity of testing (Fig. 2). We assumed that test outcome probability is a function only of whether an individual is infected and independent of other factors; one can consider this a lower bound on effectiveness of a strategy, as sensitivity and infectivity are often positively correlated with antigen testing.

To better understand the effect of rapid testing frequency and performance on healthcare capacity and mortality rates, we simulate the testing strategy with 30%-90% sensitivity each with 80% or 90% specificity against the symptomatic testing strategy (Supplementary Fig. 3).

As per our hypothesis, frequency and symptom-based testing dramatically reduced infections, simultaneous hospitalizations, and total deaths when compared to the purely symptom-based testing regiments, and infections, hospitalization, and death were reduced as frequency increased. Although testing every day was clearly most effective, even testing every fourteen days with an imperfect test gave an improvement over symptomatic testing with qRT-PCR. While the strategy works best when implemented at the very beginning of an outbreak, as demonstrated by the results in SJRP, Brazil, it also works to curb an outbreak that is already large, as demonstrated by the results in NYC. The difference between frequencies is more noticeable when the testing

274 strategy is applied to the outbreak in NYC, leading us to hypothesize that smaller outbreaks require
275 a lower testing frequency than larger ones; note the difference between the dependence on
276 frequency to curb a small initial outbreak in SJRP, Brazil versus a large one in NYC (Fig. 3).

277 For test performance of 80% sensitivity and 90% specificity, the percent of the population
278 that has been infected in total from the beginning of the outbreak to mid-July drops from 18%
279 (MA), 11% (LA), 26% (NYC), and 11% (SJRP, Brazil) to 3%, 2%, 12%, and 0.26%, respectively,
280 using a weekly rapid testing and quarantine strategy (with regards to predictions of overall
281 infection rates, other studies based on seroprevalence and epidemiological predictions have
282 reached similar conclusions [49,50]). If testing is increased to once every three days, these numbers
283 drop further to 1.6% (MA), 1.4% (LA), 9.5% (NYC), and 0.19% (SJRP, Brazil) (Table S1).

284 To further examine the relationship between frequency and sensitivity, we modeled the
285 maximum number of individuals in a given state over the 105-day time period for four geographic
286 regions (Fig. 3, Supplementary Fig. 4). In all four geographic regions, as frequency of testing
287 increases, the total infections, maximum simultaneous hospitalizations, and total deaths converge
288 to small percentages regardless of the sensitivity at high frequencies. It is clear that the difference
289 in frequency required to achieve the same result using tests of differing sensitivities is very small.
290 For example, we predict that for the outbreak in LA, a testing strategy started on 1 April of every
291 10 days using a test of sensitivity 90% would have resulted in 2.5% of the population having been
292 infected, while using a test of sensitivity 30% would require a strategy of every 5 days to achieve
293 the same number. Thus, we conclude that frequency is more important than sensitivity in curbing
294 the spread, and a large range of sensitivities prove effective when testing sufficiently often
295 (Supplementary Fig. 4)[29,51]. The following subsection contains a discussion of a location-based
296 method for varying the exact frequency of testing based on evolving outbreaks. Frequency of

297 testing can be significantly reduced to effectively contain the disease once the initial outbreak has
298 been controlled; it is clear that this takes only a matter of weeks (Fig. 2).

299 On the other hand, according to the specificity of the rapid test and the quarantine duration,
300 larger testing frequency result in a larger percent of the population quarantined (Fig. 2). Assuming
301 a 90% rapid test specificity and 10-day quarantine duration, for the 1-, 3- and 7-day frequencies
302 almost 48%, 24% and 12% of the population, respectively, would be quarantined. This figure may
303 be reduced with additional rules for exiting quarantine early, such as after complementary testing.
304 An example of such a strategy is that individuals who test positive are required to either quarantine
305 for two weeks or produce two consecutive negative rapid tests in the two days following their
306 positive result. Assuming 80% sensitivity and 90% specificity, those individuals will reenter the
307 public while still infected with probability 0.04. If uninfected, that individual will exit quarantine
308 after two days with probability 0.81. However, a compromise between the reduction of infections
309 and the proportion of the population in quarantine would be part of the planning for the appropriate
310 testing protocol in each community or region.

311 Additionally, while high frequency may be necessary to contain a large outbreak initially,
312 relatively infrequent testing, such as every one or two weeks, is sufficient to keep controlled
313 outbreaks small, while reducing the number of quarantined individuals to less than 10% of the
314 population using a two-week mandatory quarantine.

315

316 **A County-Based Testing Strategy Offers a Cost-effective Approach to Large-scale COVID-**
317 **19 Surveillance**

318 To examine the effects of resource-strategic testing schemes, we modeled the COVID-19
319 prevalence by varying testing frequency across counties of California. For this analysis, only
320 California was analyzed because of the accessibility of the county level data and the variability of

spread dynamics of the outbreaks between counties. In this scheme, the percent of active infected detected individuals in a county determines the frequency of testing. We define thresholds for the number of active detected infections that, when hit, initiate testing protocols of different frequencies depending on the threshold hit. We first tested evenly spaced thresholds for the number of detected active infections up to 1% of the population, but later adopted thresholds that were determined according to Equation 2. In Equation 2, D = population of state **D** at the time of testing. T = number of active infections which, if reached, initiates everyday testing. The days between tests are rounded to the closest integer value.

$$\text{Days between tests} = \max\left(1, 2\log_2(T/D) + 1\right) \tag{2}$$

The days between tests are chosen such that the detected active infections should remain near to or below T. If the initial detected active infections are greater than T, then the testing frequency of 1 will cause infections to rapidly drop. Both the threshold at which everyday testing begins and the coefficient of $log_2 T/D$ can be modified to produce a strategy that is more or less frequent in testing or resource effective; a range of days between tests from 14 days to 1 day are used (Fig. 4a). The purpose of this strategy is to tailor testing based on the specific characteristics of local outbreaks in order to mitigate the overall spread faster and more efficiently. A scan over different choices of T is shown in Fig. 4b; the threshold we choose in Fig. 4a is 0.05% because it is successful in curbing the outbreak within the time period we consider. While the choices work for the epidemic in California at the point we start our simulations, 10 April, they do not necessarily reflect the most resource effective choices everywhere. Our analysis could be redone to select the best fine-grained strategy in other states or metropolitan areas. The cost analysis is based only on cost per test ($7 per rapid test and $100 per PCR test) times number of tests. Clearly this neglects the

344 costs of storing, distributing, and administering tests, as well as monitoring incoming results. The
345 costs associated with these logistics would vary with differing policies dictating the administration
346 of rapid tests; significantly, whether they would be administered at home and the results self-
347 reported or in a testing facility or workplace for validation purposes. For example, a company
348 may choose to use the rapid tests to scan employees before allowing them to enter the workplace,
349 in a way similar (but more effective) to temperature checks. The cost of this particular application
350 would be minimal beyond the cost of the actual tests. Such costs would inevitably be greater for
351 PCR tests, which require a specialized testing facility, significant equipment, and highly trained
352 personnel.

353 Using a rapid test with a sensitivity of 80% and specificity of 90%, the county-based testing
354 with threshold 0.05% reduces the active infections from 0.94% to 0.0005%, while the uniform
355 strategy with tests administered every 7 days results in double the number of active infections (Fig.
356 4a). As the threshold is reduced, the total cost increases while the cumulative infections, maximum
357 percentage hospitalized, and cumulative deaths all decrease (Fig. 4b). Appropriate choice of
358 threshold is dependent on the severity of outbreaks in a specific region and available resources,
359 both logistically and fiscally. With regional data, such as that from California used to produce Fig.
360 4b, this study can be reproduced to calculate an efficient testing strategy that will effectively curb
361 outbreaks of differing severities in any geographic entity.

362 Strategy B in Fig. 4 consists of qRT-PCR testing uniformly applied to the highlighted
363 population with a frequency of once weekly. The average cost per person per day is just under $15.
364 Despite this frequency and the accuracy of qRT-PCR, the strategy does not succeed in curbing the
365 spread as fast as strategy A, which uses a testing sensitivity and specificity of 80% and 90%,
366 respectively, and testing frequency that vary between counties depending on the proportion of their

population that is currently infected. The total cost for strategy A is estimated at a fraction of the other at $1.53 per person per day.

DISCUSSION

In this study we examine the potential effects of a novel testing strategy to limit the spread of SARS-CoV-2 utilizing rapid antigen test screening approaches. Our clinical data and *SIDHRE-Q* modeling system demonstrate that 1) frequent rapid testing even at a range of accuracies is effective at reducing COVID-19 spread, 2) rapid antigen tests are a viable source for this strategy and diagnose the most infectious individuals, and 3) strategic geographic-based testing can optimize disease control with the amount of available resources. The public has witnessed and experienced symptomatic individuals being denied testing due to shortages, and few testing structures for asymptomatic or mildly symptomatic individuals, – a significant source of disease spread. Though several factors contributed to the stymied early response measures, such as lockdown and quarantine protocols and adherence, severe testing bottlenecks have been a significant culprit [52–54]. Early control measures have been shown to decrease lives lost by several orders of magnitude [55]. These challenges, though exacerbated during the early months of the pandemic, remain at the forefront of the public health crises.

Diagnosis of SARS-CoV-2 infection by qRT-PCR is the current standard of care, yet remains expensive and requires a laboratory and experienced personnel for sample preparations and experimentation. The turnaround time for results can be up to 10 days, preventing people from either leaving quarantine if they are negative, or delaying critical care and infecting others if they are positive [12]. This current testing scheme moreover yields incomplete surveillance data on which response efforts such as societal reopening and hospital management depend. Though qRT-PCR

390 is considered the gold-standard diagnostic method because of its high sensitivity and specificity,
391 the logistical hurdles render it unrealistic for large-scale screening.

392 As qRT-PCR remains impractical for this strategy, and rapid tests are facing regulatory
393 challenges because they do not perform with qRT-PCR-like accuracy, rapid test screening is either
394 nonexistent in several countries or symptom-based. Even under best-case assumptions, findings
395 have shown that symptom and risk-based screening strategies miss more than half of the infected
396 individuals [56]. Some have argued that the need for widespread testing is overstated due to the
397 variability in test sensitivity and specificity [57]. Here, we present alternative large-scale diagnostic
398 tools to qRT-PCR, and show that test performance, though valuable, is secondary to widespread
399 test frequency, which is enabled by accessibility and turnaround time. Furthermore, test
400 affordability is essential for the successful implementation in communities most affected by
401 infection and will to speed up the safe opening and functioning of the viral sectors of the economy.

402 Giordano et al. has modeled the evolution of SARS-CoV-2 spread, introducing a diagnosed
403 state to elucidate the importance of population-wide testing [29]. Larremore et al. has examined how
404 various test sensitivities and frequencies affect the reproductive number [21]. We build upon these
405 findings to show how in affected United States and Brazil regions, population-wide frequent and
406 rapid testing schemes, with sensitivities ranging from 30%-90%, can be more effective in curbing
407 the pandemic than a PCR-based scheme. Integrating real-world surveillance and clinical data into
408 our modeling system has allowed us to incorporate regional differences - such as variances in
409 healthcare access, state health policy and adherence, state GDP, and environmental factors - under
410 the same model. Significantly, our findings hold true across Massachusetts, New York City, Los
411 Angeles, and São José do Rio Preto, Brazil. We also present the economic considerations of these
412 testing regimes, showing that widespread rapid testing is more cost efficient than less frequent

413 qRT-PCR testing. In line with these economic considerations, our model demonstrates the
414 effectiveness of a geographic-based frequent testing regime, in which high disease prevalence
415 areas receive more frequent testing than low disease prevalence areas.

416 Since COVID-19 is known to affect certain demographics differently, modeling would
417 benefit from incorporating demographic information correlated with disease progression and
418 spread to define sub-models and sets of parameters accordingly. Age, pre-existing conditions, job
419 types, and density of population are examples of possible categories, each of which influence the
420 risk of contracting and/or dying from COVID-19. Further studies would benefit from incorporating
421 these ideas to better understand the effectiveness of rapid testing on identifying potential super
422 spreading events. Future public health prevention programs should use the proposed modeling
423 system to develop and test scenarios for precision testing and prevention.

424 Our findings also point to low-cost tools for implementation of this testing strategy, such
425 as a rapid antigen-based test for the detection of SARS-CoV-2 proteins. We show that the rapid
426 antigen tests perform with a range of accuracies under which disease spread can be dramatically
427 mitigated under our model. Notably, the sensitivity is correlated to the individual's viral load,
428 effectively diagnosing those who are potentially the most infectious with the highest accuracy. Our
429 findings are significant because rapid antigen tests are cheaper than qRT-PCR, can be mass
430 produced to millions per day, present results within 15 minutes, and can be administered by a
431 nonexpert without a lab or special equipment.

432 There are several policy implications for these findings. First, our model supports that
433 systems of high frequency rapid testing should be implemented as a first-line screening method.
434 This can be first enabled by a more holistic regulatory evaluation of rapid diagnostics, such that
435 policy emphasizes accessibility and turnaround time even under a range of accuracies. One can

436 imagine a less accurate, though rapid method of first-line screening in schools, public
437 transportation, and airports, or even at home, and a qRT-PCR-based method for second-line
438 screening (testing those who present severe symptoms or have been in contact with infected
439 individuals, testing in a clinical setting, etc). At home tests require a built-in digital reporting
440 capability[58]; rapid antigen test results can be sent to local health centers with reciprocal instructions
441 regarding updated test frequency guidelines to enable adaptive testing strategies. Second, our cost
442 analysis and rapid antigen test data present a viable and potentially more cost-effective method for
443 screening. Third, our county-based testing scheme presents a possible method for wide-scale
444 screening while optimizing resources. Future studies should investigate how this selective testing
445 strategy can be applied to different location scales to further inform health policy. Moreover,
446 though our models analyze regions in the United States and Brazil, similar testing strategies can
447 be considered globally in both resource limited and abundant settings due to the higher
448 accessibility of rapid tests compared to qRT-PCR. This model can be further tailored to the
449 pandemic course as we gain further evidence regarding SARS-CoV-2 re-infection rates.

450 We emphasize that integral to the effectiveness of diagnostic schemes is 1) the proper
451 adherence to quarantine and public health measures and 2) the combined use of a variety of
452 diagnostic methods including nucleic acid, antigen, and antibody tests. According to these models,
453 rapid antigen tests are an ideal tool for first-line screening. Clinical molecular tests such as qRT-
454 PCR are vital to the diagnostic landscape, particularly to re-test suspected cases that were negative
455 on the rapid test. Because rapid tests present a higher rate of false negatives, methods such as qRT-
456 PCR remain integral to second-line screening. Antibody tests provide important information for
457 immunity and vaccination purposes as well as epidemiological surveillance. This model also

assumes that individuals will quarantine themselves before being tested and for 10 days following a positive diagnostic result and will not be infected while waiting for the qRT-PCR results.

There are important limitations to be considered in this model. Differences in disease reporting between the geographical regions and the incomplete nature of COVID-19 surveillance data, often due to the lack of testing or delays in reporting, are not considered in the model. It is imperative that the testing results, hospitalization and death statistics, and changes in protocol are reported in real-time to scientists and policy makers so that models can be accurately tuned as the pandemic develops. Infectivity variations between individuals is also not applied to this model, and future clinical studies should gather data on asymptomatic presenting COVID-19 cases. Non-compliant quarantine behaviors and possible infections during testing waiting times are also not included in the calculations. The model also does not take into account infrastructural limitations (eg. hospital capacity) and . Though the rapid antigen test offers several advantages such as affordability, fast turnaround time, and ease of mass production, we are assuming that there are systems in place to implement frequent and safe low-cost screening across different communities and settings.

Our model underscores the need for a point-of-care or at-home test for frequent screening, particularly as lockdown restrictions ease. Regulatory agencies can work towards evaluating rapid tests to alternative standards other than comparison to high sensitivity molecular diagnostics, as our model shows that frequency and scale of testing may overcome lower sensitivities. Rather, we can refocus policy to implement first-line screening that optimizes accuracy with efficiency and equitability.

481 **METHODS**

482 **Development of Direct Antigen Rapid Tests for the Detection of SARS-CoV-2**

483 We developed a direct antigen rapid test for the detection of the nucleocapsid protein or
484 spike glycoprotein from SARS-CoV-2 in nasal or nasopharyngeal swab specimens as previously
485 described [59]. Briefly, the rapid antigen tests are immunochromatographic format with a visual
486 readout using anti-N or anti-S mouse monoclonal antibodies (E25Bio, Inc., Cambridge, MA, USA)
487 that are either coupled to 40 nm gold nanoparticles (Abcam, Cambridge, UK) or adsorbed to
488 nitrocellulose membranes (Sartorius, Goettingen, Germany). Each rapid antigen test has a control
489 area adjacent to the paper absorbent pad; the control is an anti-mouse Fc domain antibody (Leinco
490 Technologies, Fenton, MO, USA) that will capture any of the antibody-conjugated gold
491 nanoparticles to generate a control visual signal. A visual signal at the test area reflects SARS-
492 CoV-2 N or S that is "sandwiched" between an anti-N or anti-S antibody adsorbed to the
493 nitrocellulose membrane and a second anti-N or anti-S antibody covalently coupled to visible gold
494 nanoparticles.

495

496 **Validation of Direct Antigen Rapid Test for the Detection of SARS-CoV-2**

497 In a retrospective study of nasal swab specimens form human patients, we compared the
498 accuracy of the rapid antigen test for detection of SARS-CoV-2 N to the viral loads of individuals.
499 All individuals were symptomatic between 1-10 days of fever. Nasal swab specimens (n=158)
500 were tested following approved human subjects use protocols. The nasal swab specimens were
501 banked frozen from suspected patients submitted to PATH for routine COVID diagnosis. Prior to
502 using the rapid test, the nasal swab specimens were validated by qRT-PCR using the FDA EUA
503 ThermoFisher/AppliedBiosystems TaqPATH COVID-19 Combo Kit (ThermoFisher, Waltham,

504 MA USA). The primary study under which the samples and data were collected received ethical
505 clearance from the PATH Research Ethics Committee, protocol number 00004244. The nasal swab
506 specimens were de-identified, containing no demographic data, prior to analysis.

507 The nasal swabs were originally collected in 1 mL PBS, where 50 µl was mixed with 50 µl
508 of Solution Buffer (0.9% NaCl and 0.1% Triton X-100). The 100 µl mixture was then pipetted
509 onto the rapid antigen test for SARS-CoV-2 N detection and allowed to react for 15 minutes. After
510 processing of the rapid antigen test, the visual positive or negative signal was documented.

511 Additionally, in a retrospective study of nasopharyngeal swab specimens from human
512 patients, we compared the accuracy of the rapid antigen test to the viral load of individuals.
513 Nasopharyngeal swab specimens (n = 121) were tested in Brazil following approved human
514 subjects use protocols. The age of study participants ranged from 1 to 95 years with an overall
515 median of 37 years (interquartile range, 27–51 years), and 62% were female. All individuals were
516 symptomatic between 1-10 days of fever. The demographic summary of the patients are included
517 in Table S2. The nasopharyngeal swab specimens were banked refrigerated or frozen samples from
518 suspected patients submitted to the lab for routine COVID diagnosis. Prior to using the rapid test,
519 the nasopharyngeal swab samples were validated by qRT-PCR using GeneFinder™ COVID-19
520 Plus Real*Amp* Kit (OSANGHealtcare, Anyang-si, Gyeonggi-do, Republic of Korea I). The
521 primary study under which the samples and data were collected received ethical clearance from
522 the Faculdade de Medicina de São José do Rio Preto (FAMERP), protocol number
523 31588920.0.0000.5415. All excess samples and corresponding data were banked and de-identified
524 prior to the analyses.

525 Nasopharyngeal swab specimens (1 mL) were concentrated using Vivaspin 500 centrifugal
526 concentrator (Sartorius, Goettingen, Germany) at 12,000 x g for 10 minutes. The concentrated

527 nasopharyngeal swab specimen retentate was transferred to a collection tube and the rapid antigen
528 test for SARS-CoV-2 spike detection was inserted into the tube with the retentate and allowed to
529 react for 15 minutes. After processing of the rapid antigen test, the visual positive or negative
530 signal was documented.

531 Both nasal and nasopharyngeal swabs were used for the detection of SARS-CoV-2 N and
532 S, respectively. Some studies have shown higher efficacy of nasopharyngeal swabs for PCR tests;
533 the similar results between our two cohorts are likely due to the different proteins being
534 detected[60,61].

535

536 **Data for Modeling**

537 As of August 2020, the United States and Brazil have the highest number of confirmed
538 COVID-19 cases and deaths worldwide, with both countries reporting their first case on 26
539 February 202) [1]. Although several affected US regions could have been modeled, we look at data
540 from Massachusetts, New York, and Los Angeles: these regions each contained "hotspots", or
541 areas of surging COVID-19 cases, at different points in time during the pandemic and have
542 publicly available government-provided surveillance data. Our model is fit using data over 105
543 days beginning on April 1 for Fig. 2 and Fig. 3, and 105 days beginning on April 10 for Fig. 4 (see
544 "Modeling Parameters" in Methods). In order to understand the various testing proposals on a
545 global scale, we performed our clinical study in and expanded the modeling study to Brazil. The
546 specific data we use to fit our model are cumulative confirmed cases, total deaths, and number of
547 daily hospitalizations due to COVID-19. This surveillance data was retrieved from government-
548 provided online databases [62–68].

549

Modeling Parameters

Equation 1 below provides the exact differential equations governing the model.

$$
\begin{aligned}
\mathrm{d}\mathbf{S} &= & -\mathbf{S}\left(\alpha\mathbf{I}+\eta\mathbf{D}+\gamma\right) & & +\psi\mathbf{Q_U} \\
\mathrm{d}\mathbf{I} &= & -\mathbf{I}\left(\varepsilon+\lambda+\nu\right) & & +\mathbf{S}\left(\alpha\mathbf{I}+\eta\mathbf{D}\right) \\
\mathrm{d}\mathbf{D} &= & -\mathbf{D}\left(\frac{\mathbf{D}+\mathbf{I}}{\mathbf{D}}\mu+\rho\right) & & +\mathbf{I}(\nu+\varepsilon) \\
\mathrm{d}\mathbf{H} &= & -\mathbf{H}\left(\sigma+\tau\right) & & +\mu\left(\mathbf{D}+\mathbf{I}\right) \\
\mathrm{d}\mathbf{E} &= & & & +\tau\mathbf{H} \\
\mathrm{d}\mathbf{R} &= & -\gamma\mathbf{R} & & +\rho\mathbf{D}+\lambda\mathbf{I}+\sigma\mathbf{H}+\psi\mathbf{Q_R} \\
\mathrm{d}\mathbf{Q_U} &= & -\psi\mathbf{Q_U} & & +\gamma\mathbf{S} \\
\mathrm{d}\mathbf{Q_R} &= & -\psi\mathbf{Q_R} & & +\gamma\mathbf{R}
\end{aligned}
\tag{1}
$$

From Table 4 describing each parameter, note that each of their values are the inverse of the average rates at which a transition is made. Using average rates suffices given the large populations in each state; by the law of large numbers, variance in the time spent in each state is small. For example, the term $\alpha\mathbf{IS}$ in the top equation is equal to the number of new infection per day as a result of Susceptible/Undetected Infected interactions, where α is the rate of infectivity, and $\psi\mathbf{Q_U}$ is equal to the population exiting quarantine per day. The recovery rates in non-hospitalized infected states, λ and ρ, are assumed equal given that we do not possess sufficient quantitative data from the examined outbreaks to infer the point at which an infection is most often diagnosed (if it is diagnosed) or to train a model with separate states corresponding to each day of infectivity. Additionally, no matter which day of the infection a person is diagnosed, they are still required to quarantine for 10 days. This practice of assigning values to parameters is standard in epidemiological modeling [29,69].

In order to determine the numerical values of the parameters defining the flows between states, we use a least squares regression to find fits for each seven day interval. All data points within each interval and from each data set are fit collectively within each interval (the resulting

fits do not represent the mean of separately calculated fits). This procedure allows the model to take into account the time dependent nature of the parameters, which rely on factors such as social distancing regulations and changes in testing capacity. We also fit window sizes between 1 and 21 days and find that while the fit degrades with larger window size, the overall shape of the curves do not change. We choose seven days assuming policy changes take a week to become effective and that reasonably parameters can be expected to change within this time period without causing problems with overfitting. Also, the seven day window size accounts for the fact that often data is not reported as diligently over the weekend. Time series of the values of the parameters for the geographic locations discussed in this paper are included in Supplementary Fig. 5.

Given the restrictions on data available for the populations of various states, varying all of the parameters results in an over parameterized system. Therefore, a subset of the model parameters are fit while the others are either extracted from other sources; see Table 4. The fitting procedure minimizes the sum of the squared residuals of the total cases, current daily hospitalizations, cumulative deaths, and percentage of total infected individuals currently hospitalized. The first three are present in the data sets while the latter is derived from the estimates of the ratio between infected undetected to infected detected individuals from the CDC Laboratory Seroprevalence Survey Data [70]. While this ratio changes over time, the percentage of infected individuals developing severe symptoms should remain roughly constant throughout the course of the epidemic in the different locations studied.

We consider the data sets for outbreaks in MA, NYC, LA, and SJRP, Brazil [62–67]. While each location has testing and fatality information dating back to January, hospitalization data was not included until late March (for NYC and SJRP) and April (for MA and LA). Hence we begin our fitting procedure and testing strategy on 1 April for each of the data sets; by this point, the

outbreak is advanced in NYC, substantial in MA, non-negligible, but far from its peak, in LA, and in early stages in SJRP, Brazil. Starting simulations at various stages of the outbreak allows one to see the difference in results between when a testing strategy is administered.

In order to determine the effectiveness of the county-based strategy when applied to the state of California, we also fit all of the counties in California with a population greater than 1.5% of that of the entire state and with greater than zero deaths. The results do not depend on these selections, but instead suggest a practical criteria to administer limited resources. The fitting is done starting 10 April for these counties, as at this point the outbreak is sufficiently well-documented in each to successfully model. For the county-level data we compute a seven day running average of each of the data sets to which we then fit in order to smooth out fluctuations in the data, likely due to reporting, which are more significant here than in the other data sets considered, as the county populations are smaller and hence discrepancies impact the smoothness of the data more. The fits for each of the counties can be found in Supplementary Fig. 6.

As one can see from Fig. 1, these data sets are particularly not smooth, which indicates inefficiencies in reporting. Additionally, it is difficult to gauge their consistency within the dates provided or to compare between locations, as reporting mechanisms changed over time within the same locations. Despite this lack of consistency, our model and fitting mechanism was successful in reproducing the progress of the outbreak in each data set studied.

DATA AVAILABILITY

The authors confirm that the data supporting the findings of this study are available within the article and/or its supplementary materials; any other data will be made available upon request.

614 **CODE AVAILABILITY**

615 Full code can be found on github: https://github.com/badeaa3/COVID19_Rapid_Testing. The
616 code is written using python with the packages scipy, numpy, lmfit, matplotlib and plotly [71–75].

617

618 **SUPPLEMENTARY MATERIALS**

619

620 **Supplementary Table 1. Summary of results of COVID-19 outcomes in 3 US Regions and**
621 **Brazil as a result of Frequent Rapid Testing Protocol using SIDHRE-Q Model.**

622

623 **Supplementary Table 2. Demographic and clinical summary of patients evaluated by the**
624 **SARS-CoV-2 Direct Antigen Rapid Test (DART).**

625

626 **Supplementary Fig. 1. Performance of direct antigen rapid test (DART) for the detection of**
627 **SARS-CoV-2 (A) nucleocapsid protein and (B) spike glycoprotein.** Shown are the percentile
628 positive cases of the total positive population conditioned to qRT-PCR Cycle Threshold (Ct).
629 Percentile Positive ranks the samples in order of high Ct to low Ct. DART sensitivity is
630 determined by calculating true positive agreement to qRT-PCR; the plot uses an ax^b+c fit and
631 95% confidence intervals for the sensitivity.

632

633 **Supplementary Fig. 2. Graphical scheme displaying the relationships between the stages of**
634 **quarantine and infection in *SIDHRE-Q* model: Q-U**, quarantine uninfected; **S**, susceptible
635 (uninfected); **I**, infected undetected (pre-testing and infected); **D**, infected detected (infection
636 diagnosis through testing); **H**, hospitalized (infected with life threatening symptom progression);

637 **R**, recovered (healed); **E**, extinct (dead); and **Q-R**, quarantine recovered (healed but in
638 quarantine by false positive testing).
639
640 **Supplementary Fig. 3. COVID-19 Outcomes as a result of Frequent Rapid Testing Protocol**
641 **with variable test performances using *SIDHRE-Q* Model.** The Cumulative Detected Infected,
642 Hospitalized, Deceased, Active Infections, Recovered, and Quarantined are modeled over 105
643 days (top to bottom) using reported data from 4 global regions: Massachusetts, Los Angeles,
644 New York City, and São José do Rio Preto in Brazil (left to right). The COVID-19 population
645 spread and outcomes are modeled under a Rapid Testing Protocol with variable testing
646 frequencies ranging from 1-21 days between tests, and variable test performances: 90%
647 specificity with 90% sensitivity (A), 70% sensitivity (B), 50% sensitivity (C), and 30%
648 sensitivity (D); and 80% specificity with 90% sensitivity (E), 70% sensitivity (F), 50%
649 sensitivity (G), and 30% sensitivity (H). This protocol is compared to a symptom-based Rapid
650 Testing protocol and a symptom-based qRT-PCR protocol.
651
652 **Supplementary Fig. 4. Effect of Rapid Testing Protocol under variable testing sensitivities**
653 **and increasing frequency under the *SIDHRE-Q* Model.** The Cumulative Infections,
654 Maximum Simultaneously Hospitalized, and Deceased populations are modeled for
655 Massachusetts, Los Angeles, New York City, and São José do Rio Preto in Brazil. The effect of
656 increasing frequency of testing is modeled for various testing sensitivities (30%-90%) with an
657 80% specificity.
658
659

Supplementary Fig. 5. **Time series of the four fitted parameters α, ν, μ, and τ (left to right) for MA, LA, NYC, and SJRP (top to bottom).** See Table 4 in the Methods section for an explanation of the parameters. The values are extracted every seven days from data provided by the respective regions. The parameters vary significantly over time and location. Flat points occur during the seven day windows where the parameters are held constant. The fitting procedure is also outlined in the Methods section.

Supplementary Fig. 6. Time series of the three fitted pieces of data Cumulative Cases, Daily Hospitalized, and Cumulative Deaths (left to right) for each county receiving testing in CA; Ventura (2A), Stanislaus (2B), Santa Clara (2C), San Joaquin (2D), San Francisco (2E), San Diego (2F), San Bernardino (2G), Sacramento (2H), Orange (2I), Los Angeles (2J), Kern (2K), Fresno (2L), Alameda (2M). The counties included satisfy two requirements: population greater than 1.5% of the total CA population and nonzero total number of deaths at each point in time. The fitting procedure is outlined in the Methods section.

References

1. Coronavirus Disease (COVID-19) Situation Reports. https://www.who.int/emergencies/diseases/novel-coronavirus-2019/situation-reports.
2. Menkir, T. F. *et al.* Estimating the number of undetected COVID-19 cases exported internationally from all of China. *medRxiv* (2020) doi:10.1101/2020.03.23.20038331.
3. Ivorra, B., Ferrández, M. R., Vela-Pérez, M. & Ramos, A. M. Mathematical modeling of the spread of the coronavirus disease 2019 (COVID-19) taking into account the undetected infections. The case of China. *Commun Nonlinear Sci Numer Simul* 105303 (2020) doi:10.1016/j.cnsns.2020.105303.

684 4. Salathé, M. *et al.* COVID-19 epidemic in Switzerland: on the importance of testing, contact tracing and
685 isolation. *Swiss Med Wkly* **150**, w20225 (2020).
686 5. Lau, H. *et al.* Evaluating the massive underreporting and undertesting of COVID-19 cases in multiple global
687 epicenters. *Pulmonology* (2020) doi:10.1016/j.pulmoe.2020.05.015.
688 6. Silverman, J. D., Hupert, N. & Washburne, A. D. Using influenza surveillance networks to estimate state-
689 specific prevalence of SARS-CoV-2 in the United States. *Science Translational Medicine* (2020)
690 doi:10.1126/scitranslmed.abc1126.
691 7. Böhning, D., Rocchetti, I., Maruotti, A. & Holling, H. Estimating the undetected infections in the Covid-19
692 outbreak by harnessing capture-recapture methods. *Int. J. Infect. Dis.* **97**, 197–201 (2020).
693 8. Phipps, S. J., Grafton, R. Q. & Kompas, T. Robust estimates of the true (population) infection rate for COVID-
694 19: a backcasting approach. *Royal Society Open Science* **7**, 200909.
695 9. Guglielmi, G. The explosion of new coronavirus tests that could help to end the pandemic. *Nature* **583**, 506–
696 509 (2020).
697 10. Thebault, R. *et al.* Hospitalizations set new record as U.S. toll nears 250,000. *Washington Post*.
698 11. Wu, K. J. 'It's Kitchen Sink Time': Fast, Less-Accurate Coronavirus Tests May Be Good Enough. *The New*
699 *York Times* (2020).
700 12. Mervosh, S. & Fernandez, M. 'It's Like Having No Testing': Coronavirus Test Results Are Still Delayed. *The*
701 *New York Times* (2020).
702 13. Wang, Y. *et al.* Kinetics of viral load and antibody response in relation to COVID-19 severity. *J Clin Invest*
703 **130**, 5235–5244 (2020).
704 14. Xu, T. *et al.* Clinical features and dynamics of viral load in imported and non-imported patients with COVID-
705 19. *Int J Infect Dis* **94**, 68–71 (2020).
706 15. Zhou, R. *et al.* Viral dynamics in asymptomatic patients with COVID-19. *Int J Infect Dis* **96**, 288–290 (2020).
707 16. Hu, Z. *et al.* Clinical characteristics of 24 asymptomatic infections with COVID-19 screened among close
708 contacts in Nanjing, China. *Sci China Life Sci* **63**, 706–711 (2020).
709 17. Gao, Z. *et al.* A Systematic Review of Asymptomatic Infections with COVID-19. *J Microbiol Immunol Infect*
710 (2020) doi:10.1016/j.jmii.2020.05.001.

711 18. He, X. *et al.* Temporal dynamics in viral shedding and transmissibility of COVID-19. *Nat. Med.* **26**, 672–675
712 (2020).
713 19. Baek, Y. H. *et al.* Development of a reverse transcription-loop-mediated isothermal amplification as a rapid
714 early-detection method for novel SARS-CoV-2. *Emerg Microbes Infect* **9**, 998–1007 (2020).
715 20. Covid-19 National Testing & Tracing Action Plan. *The Rockefeller Foundation*
716 https://www.rockefellerfoundation.org/national-covid-19-testing-and-tracing-action-plan/.
717 21. Larremore, D. B. *et al.* Test sensitivity is secondary to frequency and turnaround time for COVID-19
718 surveillance. *medRxiv* (2020) doi:10.1101/2020.06.22.20136309.
719 22. Rethinking Covid-19 Test Sensitivity — A Strategy for Containment | NEJM.
720 https://www.nejm.org/doi/10.1056/NEJMp2025631?url_ver=Z39.88-
721 2003&rfr_id=ori:rid:crossref.org&rfr_dat=cr_pub%20%200pubmed.
722 23. Leo, L. Mylab gets commercial approval from ICMR for Covid-19 antigen rapid testing kit. *Livemint*
723 https://www.livemint.com/news/india/mylab-gets-commercial-approval-from-icmr-for-covid-19-antigen-rapid-
724 testing-kit-11595434040321.html (2020).
725 24. Dey, S. Coronavirus testing: Rapid antigen tests now make up nearly half of daily checks | India News - Times
726 of India. *The Times of India* https://timesofindia.indiatimes.com/india/rapid-antigen-tests-now-make-up-nearly-
727 half-of-daily-checks/articleshow/77340459.cms.
728 25. Vogels, C. B. F. *et al.* Analytical sensitivity and efficiency comparisons of SARS-CoV-2 RT-qPCR primer-
729 probe sets. *Nat Microbiol* (2020) doi:10.1038/s41564-020-0761-6.
730 26. Shen, Z. *et al.* Superspreading SARS events, Beijing, 2003. *Emerging Infect. Dis.* **10**, 256–260 (2004).
731 27. Peiris, J. S. M. *et al.* Clinical progression and viral load in a community outbreak of coronavirus-associated
732 SARS pneumonia: a prospective study. *Lancet* **361**, 1767–1772 (2003).
733 28. Bullard, J. *et al.* Predicting infectious SARS-CoV-2 from diagnostic samples. *Clin. Infect. Dis.* (2020)
734 doi:10.1093/cid/ciaa638.
735 29. Giordano, G. *et al.* Modelling the COVID-19 epidemic and implementation of population-wide interventions in
736 Italy. *Nat. Med.* **26**, 855–860 (2020).
737 30. Choi, S. & Ki, M. Estimating the reproductive number and the outbreak size of COVID-19 in Korea. *Epidemiol*
738 *Health* **42**, e2020011 (2020).

739 31. Wei, Y. Y. *et al.* [Fitting and forecasting the trend of COVID-19 by SEIR(+CAQ) dynamic model]. *Zhonghua*
740 *Liu Xing Bing Xue Za Zhi* **41**, 470–475 (2020).
741 32. Yang, Z. *et al.* Modified SEIR and AI prediction of the epidemics trend of COVID-19 in China under public
742 health interventions. *J Thorac Dis* **12**, 165–174 (2020).
743 33. Cao, S., Feng, P. & Shi, P. [Study on the epidemic development of COVID-19 in Hubei province by a modified
744 SEIR model]. *Zhejiang Da Xue Xue Bao Yi Xue Ban* **49**, 178–184 (2020).
745 34. Huang, R., Liu, M. & Ding, Y. Spatial-temporal distribution of COVID-19 in China and its prediction: A data-
746 driven modeling analysis. *J Infect Dev Ctries* **14**, 246–253 (2020).
747 35. Godio, A., Pace, F. & Vergnano, A. SEIR Modeling of the Italian Epidemic of SARS-CoV-2 Using
748 Computational Swarm Intelligence. *Int J Environ Res Public Health* **17**, (2020).
749 36. Gatto, M. *et al.* Spread and dynamics of the COVID-19 epidemic in Italy: Effects of emergency containment
750 measures. *Proc. Natl. Acad. Sci. U.S.A.* **117**, 10484–10491 (2020).
751 37. Hou, C. *et al.* The effectiveness of quarantine of Wuhan city against the Corona Virus Disease 2019 (COVID-
752 19): A well-mixed SEIR model analysis. *J. Med. Virol.* **92**, 841–848 (2020).
753 38. Zhou, T. *et al.* Preliminary prediction of the basic reproduction number of the Wuhan novel coronavirus 2019-
754 nCoV. *J Evid Based Med* **13**, 3–7 (2020).
755 39. Reno, C. *et al.* Forecasting COVID-19-Associated Hospitalizations under Different Levels of Social Distancing
756 in Lombardy and Emilia-Romagna, Northern Italy: Results from an Extended SEIR Compartmental Model. *J*
757 *Clin Med* **9**, (2020).
758 40. Tom, M. R. & Mina, M. J. To Interpret the SARS-CoV-2 Test, Consider the Cycle Threshold Value. *Clinical*
759 *Infectious Diseases* **71**, 2252–2254 (2020).
760 41. Yu, F. *et al.* Quantitative Detection and Viral Load Analysis of SARS-CoV-2 in Infected Patients. *Clin. Infect.*
761 *Dis.* **71**, 793–798 (2020).
762 42. Rao, S. N., Manissero, D., Steele, V. R. & Pareja, J. A Narrative Systematic Review of the Clinical Utility of
763 Cycle Threshold Values in the Context of COVID-19. *Infect Dis Ther* 1–14 (2020) doi:10.1007/s40121-020-
764 00324-3.

43. CDC & CDC. Options to Reduce Quarantine for Contacts of Persons with SARS-CoV-2. *Centers for Disease Control and Prevention* https://www.cdc.gov/coronavirus/2019-ncov/more/scientific-brief-options-to-reduce-quarantine.html (2020).

44. Alizargar, J. Risk of reactivation or reinfection of novel coronavirus (COVID-19). *J. Formos. Med. Assoc.* **119**, 1123 (2020).

45. Batisse, D. *et al.* Clinical recurrences of COVID-19 symptoms after recovery: viral relapse, reinfection or inflammatory rebound? *J. Infect.* (2020) doi:10.1016/j.jinf.2020.06.073.

46. Deng, W. *et al.* Primary exposure to SARS-CoV-2 protects against reinfection in rhesus macaques. *Science* (2020) doi:10.1126/science.abc5343.

47. Ota, M. Will we see protection or reinfection in COVID-19? *Nat. Rev. Immunol.* **20**, 351 (2020).

48. Victor Okhuese, A. Estimation of the Probability of Reinfection With COVID-19 by the Susceptible-Exposed-Infectious-Removed-Undetectable-Susceptible Model. *JMIR Public Health Surveill* **6**, e19097 (2020).

49. Gu, Y. COVID-19 Projections Using Machine Learning. *COVID-19 Projections Using Machine Learning* https://covid19-projections.com/.

50. Stadlbauer, D. *et al.* Seroconversion of a city: Longitudinal monitoring of SARS-CoV-2 seroprevalence in New York City. *medRxiv* 2020.06.28.20142190 (2020) doi:10.1101/2020.06.28.20142190.

51. Paltiel, A. D., Zheng, A. & Walensky, R. P. *COVID-19 screening strategies that permit the safe re-opening of college campuses*. http://medrxiv.org/lookup/doi/10.1101/2020.07.06.20147702 (2020) doi:10.1101/2020.07.06.20147702.

52. Goodnough, A. & Shear, M. D. The U.S.'s Slow Start to Coronavirus Testing: A Timeline. *The New York Times* (2020).

53. Shear, M. D. *et al.* The Lost Month: How a Failure to Test Blinded the U.S. to Covid-19. *The New York Times* (2020).

54. Kaplan, S. & Thomas, K. Despite Promises, Testing Delays Leave Americans 'Flying Blind'. *The New York Times* (2020).

55. de Souza, W. M. *et al.* Epidemiological and clinical characteristics of the COVID-19 epidemic in Brazil. *Nature Human Behaviour* **4**, 856–865 (2020).

792 56. Gostic, K., Gomez, A. C., Mummah, R. O., Kucharski, A. J. & Lloyd-Smith, J. O. Estimated effectiveness of
793 symptom and risk screening to prevent the spread of COVID-19. *eLife* **9**, e55570 (2020).
794 57. Zitek, T. The Appropriate Use of Testing for COVID-19. *West J Emerg Med* **21**, 470–472 (2020).
795 58. Commissioner, O. of the. Coronavirus (COVID-19) Update: FDA Authorizes First COVID-19 Test for Self-
796 Testing at Home. *FDA* https://www.fda.gov/news-events/press-announcements/coronavirus-covid-19-update-
797 fda-authorizes-first-covid-19-test-self-testing-home (2020).
798 59. Bosch, I. *et al.* Rapid antigen tests for dengue virus serotypes and Zika virus in patient serum. *Sci Transl Med* **9**,
799 (2017).
800 60. Callahan, C. *et al.* Nasal-Swab Testing Misses Patients with Low SARS-CoV-2 Viral Loads. *medRxiv* (2020)
801 doi:10.1101/2020.06.12.20128736.
802 61. Pinninti, S. *et al.* Comparing Nasopharyngeal and Mid-Turbinate Nasal Swab Testing for the Identification of
803 SARS-CoV-2. *Clin Infect Dis* (2020) doi:10.1093/cid/ciaa882.
804 62. Massachusetts Department of Public Health. COVID-19 Response Reporting. *Mass.gov*
805 https://www.mass.gov/info-details/covid-19-response-reporting.
806 63. California Department of Public Health. COVID-19 Cases - California Open Data.
807 https://data.ca.gov/dataset/covid-19-cases.
808 64. California Department of Public Health. COVID-19 Hospital Data - California Open Data.
809 https://data.ca.gov/dataset/covid-19-hospital-data.
810 65. Department of Health and Human Hygiene. COVID-19 Daily Counts of Cases, Hospitalizations, and Deaths |
811 NYC Open Data. https://data.cityofnewyork.us/Health/COVID-19-Daily-Counts-of-Cases-Hospitalizations-
812 an/rc75-m7u3.
813 66. Sao Jose do Rio Preto Public Health Office. *COVID-19 Surveillance Data, Sao Jose do Rio Preto*.
814 67. New York State Government. Daily Hospitalization Summary by Region. *New York Forward*
815 https://forward.ny.gov/daily-hospitalization-summary-region.
816 68. Massachusetts General Hospital Institute for Technology Assessment. COVID-19 Simulator - Methodology.
817 https://www.covid19sim.org/images/docs/COVID-19_simulator_methodology_download_20200507.pdf.
818 69. Kermack, W. O. & McKendrick, A. G. Contributions to the mathematical theory of epidemics—I. *Bltn Mathcal*
819 *Biology* **53**, 33–55 (1991).

70. CDC. Coronavirus Disease 2019 (COVID-19). *Centers for Disease Control and Prevention* https://www.cdc.gov/coronavirus/2019-ncov/cases-updates/commercial-lab-surveys.html (2020).
71. SciPy.org — SciPy.org. https://www.scipy.org/.
72. NumPy. https://numpy.org/.
73. Non-Linear Least-Squares Minimization and Curve-Fitting for Python — Non-Linear Least-Squares Minimization and Curve-Fitting for Python. https://lmfit.github.io/lmfit-py/.
74. Matplotlib: Python plotting — Matplotlib 3.3.1 documentation. https://matplotlib.org/.
75. Plotly: The front-end for ML and data science models. https://plotly.com/.

Acknowledgments

General: We thank Professor Lee Gehrke for critical reading of the manuscript.

Funding: EN is funded by Tufts University DISC Seed Grant. MLN is supported by a FAPESP grant (#2020/04836-0) and is a CNPq Research Fellow. AFV is supported by a FAPESP Fellow grant (#18/17647-0). GRFC is supported by a FAPESP Fellow grant (#20/07419-0). BHGAM is supported by a FAPESP Scholarship (#19/06572-2). The funders had no role in the design of the study; in the collection, analyses, or interpretation of data; in the writing of the manuscript, or in the decision to publish the results.

Author contributions: Conceptualization: BBH. Formal analysis: BN, AB, AR, MB, NS, ARG, AV, GCDS, TMILDS, BHGAM, MMM, GRFC, FQ, AFNR, MLG, ENN, IB, BBH. Funding acquisition: IB, BBH. Investigation: BN, AB, AR, MB, NS, ARG, AV, GCDS, TMILDS, BHGAM, MMM, GRFC, FQ, AFNR, MLG, ENN, IB, BBH. Methodology: BN, AB, AR, MB, NS, ARG, AV, GCDS, TMILDS, BHGAM, MMM, GRFC, FQ, AFNR, MLG, ENN, IB, BBH. Project administration: MLN, IB, BBH. Resources: MLN, IB, BBH. Supervision: MB, MLN, ENN, IB, BBH. Validation: BN,

845 AB, AR, MB, ENN, BBH. Visualization: BN, AB, AR, MB, AV, ENN, BBH. Writing—
846 original draft: AR, BBH. Writing—review and editing: BN, AB, AR, MB, NS, ARG,
847 AV, GCDS, TMILDS, BHGAM, MMM, GRFC, FQ, AFNR, MLG, ENN, IB, BBH.
848 **Competing interests:** BN, AB, AR, MB, NS, AG, IB, and BBH are employed by or
849 affiliated with E25Bio Inc. (www.e25bio.com), a company that develops diagnostics for
850 epidemic viruses.
851
852
853
854
855
856
857
858
859
860
861
862
863
864
865
866
867

868 **Figures and Tables**

869

870 **TABLES**

871 **Table 1. Data summary of direct antigen rapid test (DART) for detection of SARS-CoV-2**
872 **nucleocapsid protein and DART for detection of SARS-CoV-2 spike glycoprotein**
873 **performance in comparison to qRT-PCR results.** Sensitivity, specificity, Positive predicative
874 value, (PPV) negative predictive value (NPV), prevalence, and overall agreement are calculated
875 for increasing PCR cycle threshold (Ct) values.

876

877

		Cycle threshold (Ct) value	Total Cases	DART Positives	DART Negatives	Sensitivity	95% Confidence Interval	Specificity	95% Confidence Interval	Positive Predictive Value (PPV)	Negative Predictive Value (NPV)
DART (nucleocapsid protein)	SARS-CoV-2 (Gene Average)	< 20	82	24	58	95.8%	78.9%-99.9%	100.0%	93.8%-100%	100.0%	98.3%
		< 25	111	53	58	92.5%	81.8%-97.9%	100.0%	93.8%-100%	100.0%	93.5%
		< 30	136	78	58	85.9%	76.2%-92.7%	100.0%	93.8%-100%	100.0%	84.1%
		< 35	157	99	58	81.8%	72.8%-88.9%	100.0%	93.8%-100%	100.0%	76.3%
		< 40	158	100	58	82.0%	73.1%-89.0%	100.0%	93.8%-100%	100.0%	76.3%
DART (spike glycoprotein)	SARS-CoV-2 (Gene Average)	< 10	51	2	49	100.0%	20.9%	85.7%	4.9%	22.2%	98.9%
		< 15	72	23	49	100.0%	2.8%	85.7%	4.9%	76.7%	98.9%
		< 20	90	41	49	97.6%	2.8%	85.7%	4.9%	85.1%	96.6%
		< 25	111	62	49	91.9%	3.4%	85.7%	4.9%	89.1%	89.4%
		< 30	121	72	49	84.7%	4.1%	85.7%	4.9%	89.7%	79.2%
		< 35	121	72	49	84.7%	4.1%	85.7%	4.9%	89.7%	79.2%

878 **Table 2. Clinical validation summary for the direct antigen rapid test (DART) for SARS-**

879 **CoV-2 nucleocapsid protein evaluated using 158 retrospectively collected patient nasal**

880 **swab specimens.**

881

All Data Summary								
		qRT-PCR (gene average)					95% Confidence Interval	
		+	-	Total	Sensitivity	82.0%	73.1%	89.0%
DART (nucleocapsid protein)	+	82	0	82	Specificity	100.0%	93.8%	100.0%
	-	18	58	76	Positive Predictive Value	100.0%	93.8%	100.0%
	Total	100	58	158	Negative Predictive Value	76.3%	65.2%	85.3%
					Prevalence	63.3%	55.3%	70.8%
					Overall Agreement	88.6%	82.6%	93.1%

882

883

884

885

886

887

888

889

890

891

892 **Table 3. Clinical validation summary for the SARS-CoV-2 direct antigen rapid test**

893 **(DART) for SARS-SoC-2 spike glycoprotein evaluated using 121 retrospectively collected**

894 **patient nasopharyngeal swab specimens.**

895

896

All Data Summary								
		qRT-PCR (gene average)					95% Confidence Interval	
		+	-	Total	Sensitivity	84.7%	80.6%	88.9%
DART (spike glycoprotein)	+	61	7	68	Specificity	85.7%	80.8%	90.6%
	-	11	42	53	Positive Predictive Value	89.7%	86.2%	93.2%
	Total	72	49	121	Negative Predictive Value	79.2%	73.6%	84.9%
					Prevalence	59.5%	53.9%	65.1%
					Overall Agreement	85.1%	82.0%	88.3%

897

898

899

900

901

902

903

904

905

906

907

Table 4. Details of parameter values used for *SIDHRE-Q* Model.

Parameter	Details & Statistics			
α	α is the probability that an interaction between an undetected infected person and an uninfected person results in a new infection, divided by the average number of uninfected people an undetected infected person comes into contact with per day. α is estimated from the data. Units: 1/(days × people).		Mean	St. Dev.
		MA	0.088	0.051
		LA	0.090	0.034
		NYC	0.067	0.042
		SJRP	0.121	0.042
η	η is the probability that an interaction between an infected person and an uninfected person results in a new infection, divided by the average number of uninfected people a detected infected person comes into contact with on a given day. Units: 1/(days × people). $\eta = 0.01 \cdot \alpha$ The constant relating η, α accounts for a small but nonzero transmission due to the quarantined (detected) infected population. This value was chosen to be small, assuming a quarantined individual will only infect others with low probability.			
ν	ν is the probability that a symptomatic undetected individual is diagnosed per day. ν is estimated from the data. ν is multiplied by sensitivity (assume benchmark sensitivity 100% for PCR, as used when fitting). Units: 1/days.		Mean	St. Dev.
		MA	0.006	0.005
		LA	0.011	0.006
		NYC	0.0056	0.002
		SJRP	0.015	0.007
ϵ	ϵ is the probability that an asymptomatic undetected infected individual is diagnosed on a given day. $\epsilon = 0$ while fitting (during PCR symptomatic testing). ϵ =(sensitivity/days between tests) when the rapid testing strategy is activated. Units: 1/days.			
λ	λ is the probability that an undetected infected individual transitions to the recovered state on a given day. $\lambda = 1/10$, or the inverse of average recovery time [68]. Units: 1/days.			
μ	μ is the probability that an infected individual develops severe symptoms on a given day and transitions into the hospitalized state. The flow from D to H is assumed to be independent of the ratio I/D, but comes only from the detected infected population, hence why it is multiplied by $(I + D)/D$. μ is estimated from the data. Units: 1/days.		Mean	St. Dev.
		MA	0.0013	9.5e-4
		LA	0.0016	2.4e-4
		NYC	0.0011	6.6e-4
		SJRP	0.0018	8.0e-4

<table>
<tr><td>ρ</td><td>ρ is the probability that a detected infected individual transitions to the recovered state on a given day.

$\rho = 1/10$, or the inverse of the average recovery time [68]. Units: 1/days.</td></tr>
<tr><td>σ</td><td>σ is the probability that a hospitalized individual transitions to the recovered state on a given day. $\sigma = 1/11$, or the inverse of the average recovery time for a hospitalized individual [68]. Units: 1/days.</td></tr>
<tr><td>τ</td><td>τ is the probability that a hospitalized individual expires on a given day. τ is estimated from the data. Units: 1/days.
<table>
<tr><td></td><td>Mean</td><td>St. Dev.</td></tr>
<tr><td>MA</td><td>0.034</td><td>0.012</td></tr>
<tr><td>LA</td><td>0.016</td><td>0.004</td></tr>
<tr><td>NYC</td><td>0.036</td><td>0.034</td></tr>
<tr><td>SJRP</td><td>0.032</td><td>0.045</td></tr>
</table></td></tr>
<tr><td>γ</td><td>γ is the probability of entering either of the quarantine states on a given day from either the Susceptible or Recovered populations. $\gamma = 0$ while fitting (during PCR symptomatic testing). $\gamma = (1 - \text{specificity}) \times (1/\text{days between tests})$ when the rapid testing strategy is activated. Units: 1/days.</td></tr>
<tr><td>ψ</td><td>ψ is the probability that an individual exits quarantine on a given day. $\psi = 1/10$, or the inverse of the quarantine period for fixed length quarantine. Units: 1/days.</td></tr>
</table>

FIGURES

Fig. 1. Graphical scheme displaying the relationships between the stages of quarantine and infection in *SIDHRE-Q* model. **Q-U**, quarantine uninfected; **S**, susceptible (uninfected); **I**, infected undetected (pre-testing and infected); **D**, infected detected (infection diagnosis through testing); **H**, hospitalized (infected with life threatening symptom progression); **R**, recovered (healed); **E**, extinct (dead); and **Q-R**, quarantine recovered (healed but in quarantine by false positive testing).

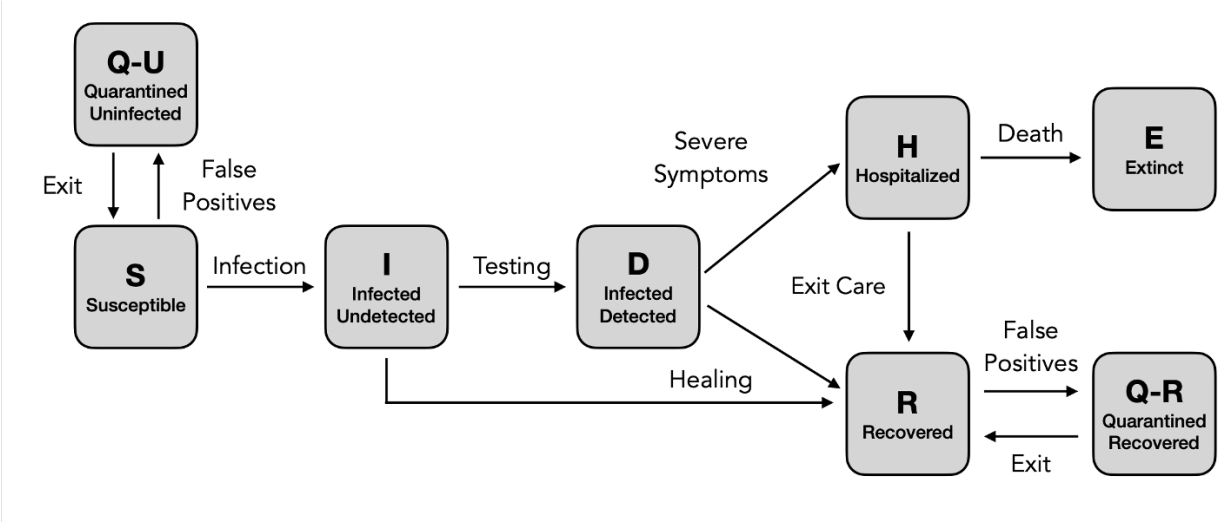

Fig. 2. COVID-19 Outcomes in 3 US Regions and Brazil as a result of Frequent Rapid Testing Protocol using the *SIDHRE-Q* Model. The Cumulative Detected Infected, Hospitalized, Deceased, Active Infections, Recovered, and Quarantined are modeled over 105 days (top to bottom) using reported data from 4 global regions: Massachusetts, Los Angeles, New York City, and São José do Rio Preto in Brazil (left to right). The COVID-19 population spread and outcomes are modeled under a Rapid Testing Protocol (sensitivity 80%, specificity 90%) with variable testing frequencies ranging from 1-21 days between tests. This protocol is compared to a symptom-based Rapid Testing protocol and a symptom-based PCR protocol.

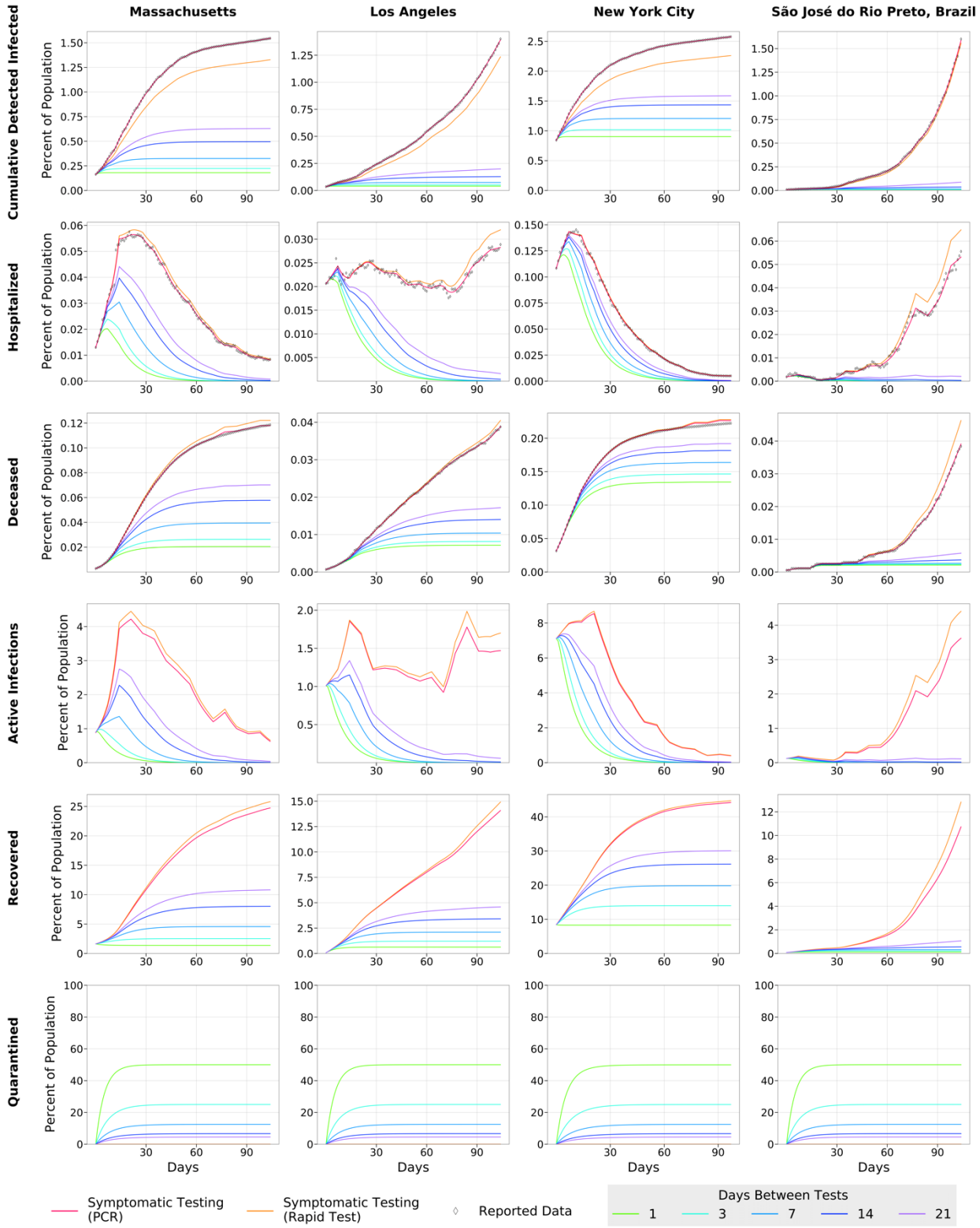

Sensitivity: 80.0% Specificity: 90.0%

Fig. 3. Effect of Rapid Testing Protocol under variable testing sensitivities (30%-90%) and increasing frequency under the *SIDHRE-Q* Model. The Cumulative Infections, Maximum Simultaneously Hospitalized, and Deceased populations are modeled for Massachusetts, Los Angeles, New York City, and São José do Rio Preto in Brazil with a 90% test specificity.

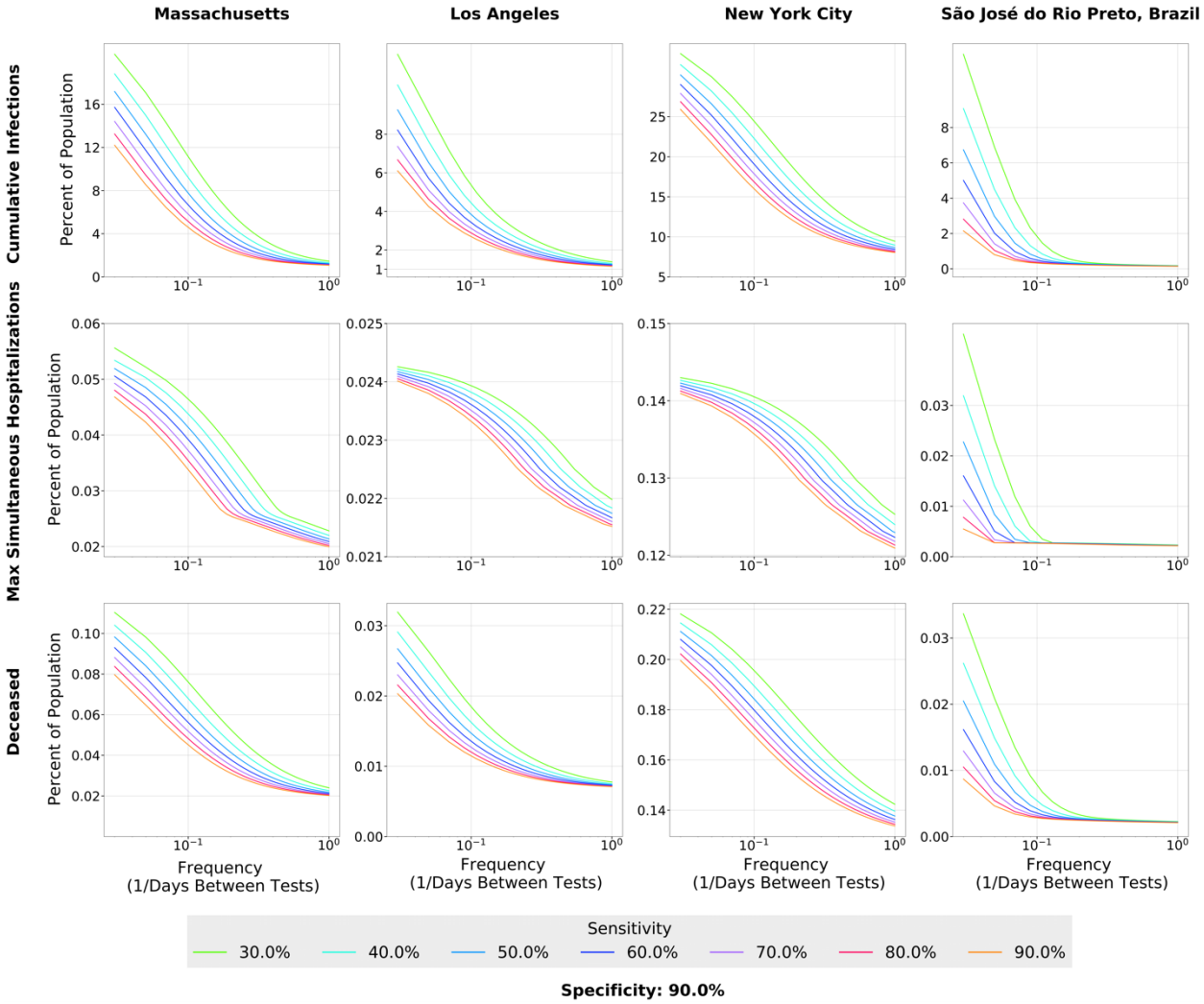

962 **Fig. 4. Effect of County Based Rapid Testing strategy on COVID-19 outcomes in**
963 **California.** This protocol varies testing frequency in accordance to the number of recorded
964 cases; the threshold for number of active infections which, if reached, signals to commence
965 everyday testing (the highest frequency considered). A Rapid Test with an 80% sensitivity and
966 90% sensitivity versus is used in this deployment strategy. Shown is the total cost per person per
967 day versus the cumulative infections, maximum simultaneously hospitalized, and cumulative
968 deaths with varied thresholds for all of CA is shown. The County Based Rapid Testing strategy
969 is compared to uniform testing, which distributes the same number of total tests used in the
970 county strategy, albeit evenly across each county. The effects of uniform testing are modeled for
971 both a Rapid Testing protocol and a qRT-PCR protocol (A). The effects of County Based Rapid
972 Test Protocol and Uniform PCR Protocol on active infected detected population over time in CA
973 are shown (B). The legend denotes the thresholds at which testing frequency is determined, the
974 testing frequencies, the percent of CA population under the strategy, and the cost per person per
975 day.
976
977
978
979
980
981
982
983
984

(A)

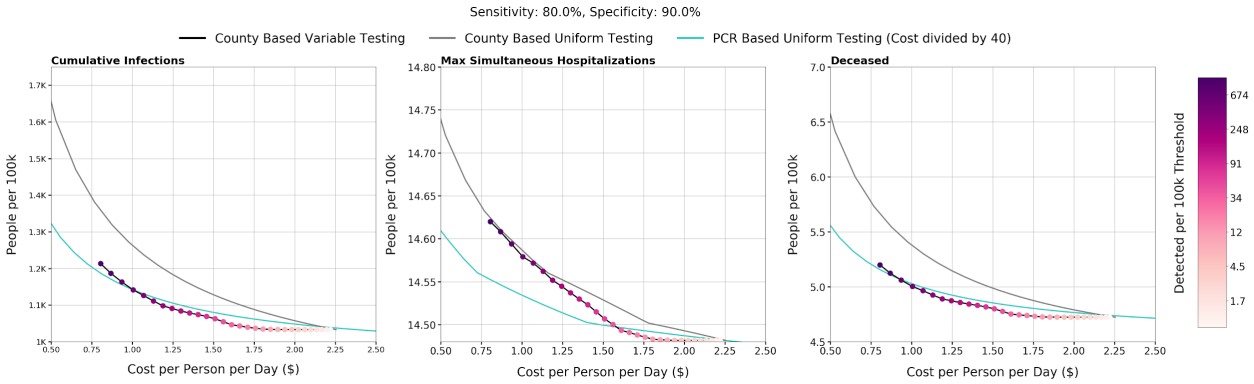
Sensitivity: 80.0%, Specificity: 90.0%
County Based Variable Testing
County Based Uniform Testing
PCR Based Uniform Testing (Cost divided by 40)
Cumulative Infections
Max Simultaneous Hospitalizations
Deceased
People per 100k
Cost per Person per Day ($)
Detected per 100k Threshold
674
248
91
34
12
4.5
1.7

(B)

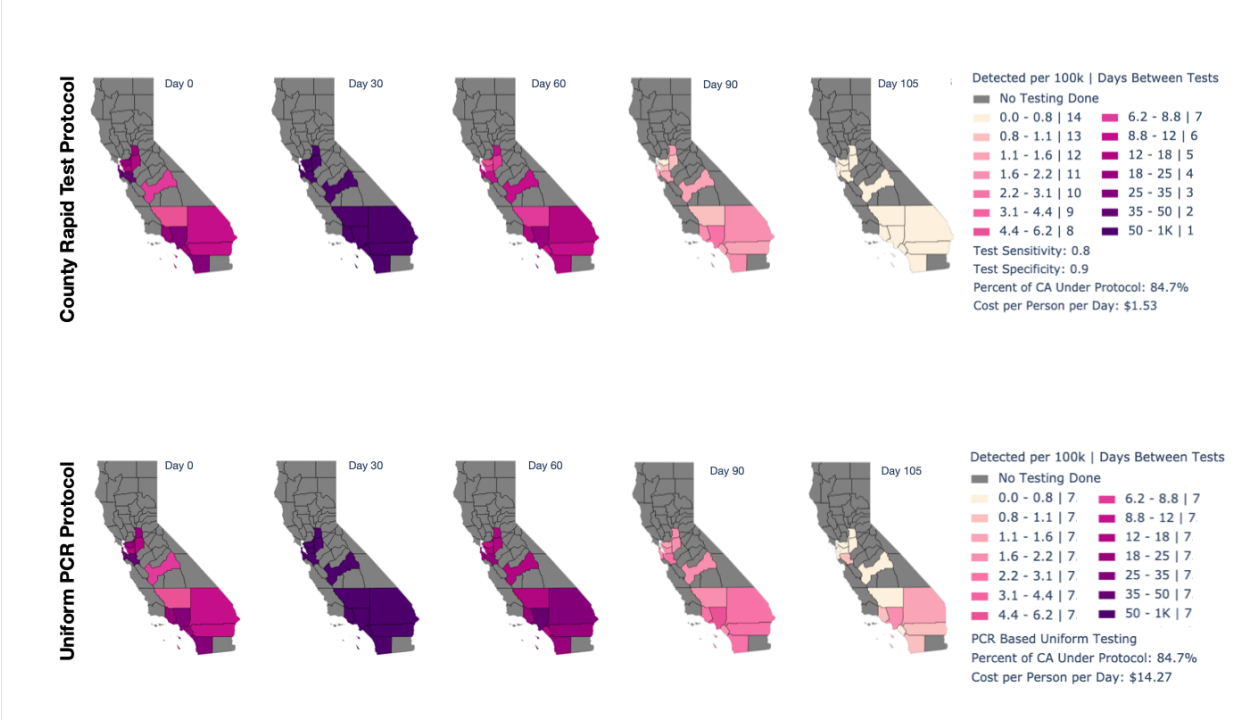
County Rapid Test Protocol
Uniform PCR Protocol
Day 0
Day 30
Day 60
Day 90
Day 105
Detected per 100k | Days Between Tests
No Testing Done
0.0 - 0.8 | 14
0.8 - 1.1 | 13
1.1 - 1.6 | 12
1.6 - 2.2 | 11
2.2 - 3.1 | 10
3.1 - 4.4 | 9
4.4 - 6.2 | 8
6.2 - 8.8 | 7
8.8 - 12 | 6
12 - 18 | 5
18 - 25 | 4
25 - 35 | 3
35 - 50 | 2
50 - 1K | 1
Test Sensitivity: 0.8
Test Specificity: 0.9
Percent of CA Under Protocol: 84.7%
Cost per Person per Day: $1.53
Detected per 100k | Days Between Tests
No Testing Done
0.0 - 0.8 | 7
0.8 - 1.1 | 7
1.1 - 1.6 | 7
1.6 - 2.2 | 7
2.2 - 3.1 | 7
3.1 - 4.4 | 7
4.4 - 6.2 | 7
6.2 - 8.8 | 7
8.8 - 12 | 7
12 - 18 | 7
18 - 25 | 7
25 - 35 | 7
35 - 50 | 7
50 - 1K | 7
PCR Based Uniform Testing
Percent of CA Under Protocol: 84.7%
Cost per Person per Day: $14.27